Differences in actionable genomic alterations between brain metastases and non-brain metastases in patients with non-small cell lung cancer

RUI NIAN[1*], HUIHUI JIANG[2*], JIANGMAN ZHAO[2*], WANLE HOU[3], HUA ZHANG[4], JIANGTAO MA[5], PENGBIAO LV[6], LISHA JIANG[2], YONGPAN WANG[2], YUE XU[2], SHOUXIN WU[2], JINGWEI LOU[2] and WANJUN LI[1]

[1]Department of Pathology, Affiliated 3201 Hospital of Xi'an Jiaotong University, Shaanxi, Hanzhong 723000; [2]Zhangjiang Center for Translational Medicine, Shanghai Biotecan Pharmaceuticals Co., Ltd., Shanghai 200135; [3]Department of Laboratory Medicine, First Hospital of Laohekou City, Hubei, Xiangyang 441800; [4]Department of Pathology, Hanzhong People's Hospital; [5]Medical Laboratory Science, Hanzhong Railway Central Hospital; [6]Department of Surgical Oncology, Hanzhong People's Hospital, Shaanxi, Hanzhong 723000, P.R. China

Received November 30, 2021; Accepted June 15, 2022

DOI: 10.3892/ijo.2022.5390

Abstract. Brain metastases (BM) have been closely associated with increased morbidity and poor survival outcomes in patients with non-small cell lung cancer (NSCLC). Excluding risk factors in histological subtypes, genomic alterations, including epidermal growth factor receptor mutations and anaplastic lymphoma kinase (*ALK*) rearrangements have been also regarded as greater risk factors for BM in the aspect of molecular subtypes. In the present study, 69 tumor tissues and 51 peripheral blood samples from patients with NSCLC were analyzed using a hybridization capture-based next-generation sequencing (NGS) panel, including 95 known cancer genes. Among the 90 patients with stage IV NSCLC, 26 cases suffered from BM and 64 cases did not. In total, 174 somatic mutations in 35 mutated genes were identified, and 12 of these genes were concurrently present in the BM group and the non-BM group. Importantly, five mutated genes including *ALK*, cytidine deaminase (*CDA)*, SMAD family member 4 (*SMAD4)*, superoxide dismutase 2 (*SOD2*) and Von Hippel-Lindau tumor suppressor (*VHL*) genes were uniquely detected in the BM group, and they were enriched in the Hippo signaling pathway, pyrimidine metabolism and pantothenate and co-enzyme A (CoA) biosynthesis, as demonstrated using Kyoto Encyclopedia of Genes and Genomes enrichment analysis. RNA polymerase II transcription regulator complex and promyelocytic leukemia nuclear body were the top functional categories according to the Gene Ontology enrichment analysis in the BM group and non-BM group, respectively. Furthermore, 43.33% (13/30) of mutated genes were detected by both tumor tissue deoxyribonucleic acid (DNA) and plasma-derived circulating tumor DNA (ctDNA) in the non-BM group, while this percentage was only limited to 29.41% (5/17) in the BM group. To summarize, significant differences in somatic mutations, somatic interactions, key signaling pathways, functional biological information, and clinical actionability for the therapy of targeted agents were founded between the BM group and the non-BM group, and ctDNA analysis may by applied as a more credible alternative for genomic profiling in patients with advanced NSCLC without BM, due to its higher consistency for genomic profiling between ctDNA analysis and tissue DNA analysis.

Correspondence to: Professor Wanjun Li, Department of Pathology, Affiliated 3201 Hospital of Xi'an Jiaotong University, 783 Tianhan Avenue, Shaanxi, Hanzhong 723000, P.R. China
E-mail: lwjdf163@163.com

Dr Jingwei Lou, Zhangjiang Center for Translational Medicine, Shanghai Biotecan Pharmaceuticals Co., Ltd., 180 Zhangheng Road, Shanghai 200135, P.R. China
E-mail: jingweilou@biotecan.com

*Contributed equally

Key words: non-small cell lung cancer, brain metastases, tissue, circulating tumor deoxyribonucleic acid, somatic mutations

Introduction

Brain metastases (BM) can be detected in 10-20% of patients with non-small cell lung cancer (NSCLC) at the initial diagnosis and the percentage extends up to 50% during disease progression (1-3). The development of BM leads to an evident incidence of neurocognitive and functional deficits in patients with NSCLC, which adversely affects the quality of life (4). BM is closely related to a poor prognosis, and the median overall survival (OS) of patients with NSCLC with BM is limited only up to 4-6 months (5,6). However, the molecular mechanisms underlying the high morbidity, poor prognosis, and high mortality rate of patients with NSCLC with BM remain largely unknown.

In terms of histological subtypes, BM occurs most frequently in patients with lung adenocarcinoma (54 and 58.6%), as compared to non-adenocarcinoma subtypes

(large cell carcinoma, 17.7%; and squamous cell carcinoma, 9.9%) (7,8). Moreover, patients with NSCLC harboring epidermal growth factor receptor (*EGFR*) mutations or anaplastic lymphoma kinase (*ALK*) rearrangements are at a greater risk of developing BM, in the aspect of molecular subtypes (9,10). Pathogenic driver mutations have been reported to be vital for therapeutic decision-making, since targeted therapies significantly improve survival outcomes for the majority of patients (11). Specifically, a subgroup of patients with BM responds well to *EGFR* tyrosine kinase inhibitors (*EGFR*-TKIs) (12). However, actionable genomic alterations are not currently available for recurrent or progressive diseases, due to the unsafety of the invasive biopsy procedure and/or the inaccessibility of tumor sites, particularly for patients with BM. Currently, knowledge about pathogenic driver mutations is most frequently obtained from primary or metastatic tumor tissue at easily accessible sites; however, a divergent mutation landscape from these sites has been observed (13,14). Thus, safe, convenient and replaceable approaches are essential to acquiring genomic characterization for patients with NSCLC with BM.

Liquid biopsy is regarded as a promising minimally-invasive approach to obtaining tumor cells, as opposed to invasive tissue biopsies in molecular diagnostics in recent years (15). Cell-free deoxyribonucleic acid (cfDNA), which has been previously detected in blood and body fluids, is released from cells when they undergo necrosis, apoptosis and lysis (16,17). Circulating tumor DNA (ctDNA), the tumor-derived fraction of cfDNA, possesses the potential ability to represent the whole tumor burden across different metastatic sites, partly circumventing tumor spatial heterogeneity issues (18). Since the reliability of a single-tumor tissue biopsy for the obtainment of the whole mutation landscape, the limitations of personalized medicine approaches are a dilemma. Multiregional biopsy analysis has already been proposed by Gerlinger *et al* (19), in order to profile a more complete mutation landscape and predict the therapeutic outcome. Additionally, several studies have suggested that a dynamic sampling of somatic mutations from ctDNA analysis may represent a larger clonal hierarchy (20-23), rendering the realization of therapeutic decisions and tracking therapeutic outcomes safer and more convenient, even across different metastatic sites.

In the present study, targeted next-generation sequencing (NGS) of tumor tissues and peripheral blood samples from patients with NSCLC was conducted, using a hybridization capture-based panel consisting of 95 known cancer genes. The present study aimed to identify the characteristic of genomic alternations in patients with advanced NSCLC with or without BM. The novelty of the present study was, to the best of our knowledge, systematical comparisons of the differences in somatic mutations, somatic interactions, key signaling pathways, functional biological information and clinical actionability for the therapy of targeted agents between the BM group and the non-BM group. The findings presented herein may possibly aid towards the elucidation of the underlying molecular mechanisms underlying the initiation or progression of BM in NSCLC. Furthermore, it was also investigated whether ctDNA analysis may serve as a more credible alternative for genomic profiling in patients with advanced NSCLC with BM than in patients without BM.

Patients and methods

Patients and sample collection. In total, 120 patients with NSCLC from the Department of Pathology at the Affiliated 3201 Hospital of Xi'an Jiaotong University were recruited between May, 2017 and December, 2020. The pathological diagnosis was verified by three pulmonary pathologists, based on the 4th edition of the World Health Organization Classification of Lung Tumors (24). Tumors with histological components other than NSCLC were excluded. In total, one fresh tumor tissue, 68 formalin-fixed and paraffin-embedded (FFPE) tumor specimens and 51 peripheral blood specimens were collected for next-generation sequencing (NGS) analysis. Written informed consent was acquired from all participating individuals. The study was performed according to the Code of Ethics of the World Medical Association (Declaration of Helsinki) (25), and it was approved by the Medical Ethics Committee of Affiliated 3201 Hospital of Xi'an Jiaotong University. The corresponding Institutional Review Board (IRB) number was No.008(2017).

DNA extraction and quality control. Genomic DNA (gDNA) from fresh tumor tissues, FFPE tumor specimens and plasma was extracted using the QIAamp DNA Mini kit (Qiagen GmbH), GeneRead DNA FFPE kit (Qiagen GmbH) and the HiPure Circulating DNA Midi kit C (Magen Biotechnology Co., Ltd.), respectively. The Qubit® 3.0 Fluorometer (Invitrogen; Thermo Fisher Scientific, Inc.) and NanoDrop ND-1000 (Thermo Scientific, Inc.) were used for the quantity and purity evaluation of the gDNA. The fragmentation status was evaluated using the Agilent 2100 Bioanalyzer instrument (Agilent Technologies, Inc.) with the High Sensitivity DNA Reagent (Agilent Technologies, Inc.) to produce a DNA integrity number. Additionally, the step of quality control (QC) was also performed to evaluate FFPE DNA integrity by multiplex Polymerase Chain Reaction (PCR). In brief, gDNA (30 ng) was amplified using three different primers of the glyceraldehyde-3-phosphate dehydrogenase (*GAPDH*) gene, sized at 200-400 base pairs (Table SI). The Agilent 2100 Bioanalyzer instrument (Agilent Technologies, Inc.) was used to determine the concentration of multiplex PCR products. The fragmentation of gDNA from FFPE was estimated by the average yield ratio (AYR) value, which was calculated by dividing the yield ratio of reference DNA (Promega Corporation) by each amplicon's yield ratio.

Library preparation and hybridization capture. In total, 300 ng gDNA from each sample was mechanically fragmented using an E220 focused ultrasonicator Covaris (Covaris, LLC.). The targeted size of the DNA fragment was between 150 and 200 bp. Subsequently, 10-100 ng DNA was used for library construction with the KAPA library preparation kit (Kapa Biosystems Inc.; Roche Diagnostics), which was constructed with end-repair, A-tailing and adapter ligation without additional fragmentation, according to the manufacturer's instructions. Finally, the NGS libraries were captured using the xGen Lockdown Probe pool (Integrated DNA Technologies, Inc.), and the captured DNA fragments were amplified for 13 cycles of PCR, using 1X KAPA HiFi Hot Start Ready Mix (Kapa Biosystems Inc.; Roche Diagnostics). The thermal cycling conditions used were as follows: Initial

denaturation for 45 sec at 98˚C followed by 13 cycles of 98˚C for 15 sec, 60˚C for 30 sec, and 72˚C for 30 sec. The final extension was performed at 72˚C for 60 sec.

Illumina sequencing. Following QC and quantification using the Agilent 2100 Bioanalyzer (Agilent Technologies, Inc.) and Qubit® 3.0 Fluorometer (Invitrogen; Thermo Fisher Scientific, Inc.), the NGS libraries were sequenced on an Illumina NextSeq CN500 platform with a medium flux chip (NextSeq CN500 Mid Output v2 kit; Illumina Inc.).

Bioinformatics analysis. Clean data were obtained following filtering low-quality reads, which includes reads with adapter sequences and reads with length <36 bp. All filtered reads were aligned to the human genome (University of California Santa Cruz ID: hg19) using the Burrows-Wheeler-Alignment Tool (BWA v.0.7.12; Wellcome Trust Sanger Institute) (26). Subsequently, the Picard and Genome Analysis Toolkit (GATK v.3.2; Broad Institute) method was used for duplicate removal, local realignment, and base quality score recalibration, and it was also adopted for generating quality statistics, including mapped reads, mean mapping quality, and mean coverage. Finally, the VarDict (v.1.6.0; GitHub, Inc.) was adopted for the identification of single nucleotide variation (SNV) and Insertion/Deletion (InDel) (27).

The ANNOVAR software tool (v. 20210202; https://annovar.openbioinformatics.org/en/latest/) was used for annotating somatic variants (28). The candidates of somatic variants were identified by the following filter conditions: i) Removal of the variants coverage depth (VDP) <10; ii) removal of the variant sites with mutant allele frequency (MAF) >0.001 in the 1,000 Genomes databases (1,000 Genomes Project Consortium; https://www.internationalgenome.org/) and Exome Aggregation Consortium (ExAC) (https://ncbiinsights.ncbi.nlm.nih.gov/tag/exac/); iii) retainment of variant sites with MAF≥0.001 and <0.1 in the 1,000 Genomes databases with COSMIC evidence (http://cancer.sanger.ac.uk/cosmic); iv) retainment of variations in the exon or splicing region (10 bp upstream and downstream of splicing sites); v) remove synonymous mutations; vi) remove unknown variant classification; and vii) removal of the functional benign variant sites, predicted by PolyPhen-2 (Polymorphism Phenotyping v2; http://genetics.bwh.harvard.edu/pph2/) (29) or MutationTaster (MutationTaster2020; https://www.mutationtaster.org/) (30). Additionally, the association between the identified somatic mutations and their clinical significance was established by OncoKB Precision Oncology Database (http://oncokb.org/). Kyoto Encyclopedia Of Genes and Genomes (KEGG) and Gene Ontology (GO) enrichment analysis were used to explore the biological consequences of mutant genes by using the cluster Profiler package (http://bioconductor.org/packages/release/bioc/html/clusterProfiler.Html) in R software (R 4.0.3, R Core Team; https://www.RProject.org) (31).

Statistical analysis. The maftools package in R software (R 4.0.3, R Core Team; https://www.R-Project.org) was used to create somatic mutation landscapes, co-Barplots, co-Oncoplots, lollipop plots, and spectrums of co-occurring and mutually exclusive genomic alterations. Fisher's exact test was used to evaluate the statistical differences in categorical variables between the BM group and the non-BM group using R software (R 4.0.3, R Core Team; https://www.RProject.org). Statistical analyses were two-sided, and P<0.05 was considered to indicate a statistically significant difference.

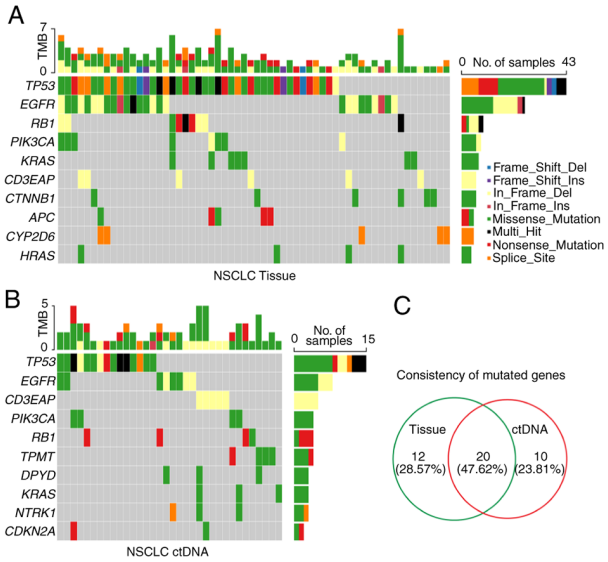

Figure 1. The landscape of somatic mutation in patients with NSCLC from (A) tumor tissue DNA (n=69) and (B) ctDNA (n=51). (C) Venn diagram of mutated genes derived from tissue DNA analysis or ctDNA analysis. Mutated genes are ranked by mutation frequency. The bars on the right represent the mutation frequencies of each gene. TMB (mutations per Mb) is demonstrated in the upper panel. Patients were arranged along the x-axis. NSCLC, non-small cell lung cancer; ctDNA, circulating tumor DNA; TMB, tumor mutation burden.

Results

Patient characteristics. In the present retrospective study, the numbers of patients with different stages of NSCLC were as follows: I, II, III and IV were as follows: i) Stage I, 6 patients (aged 61-78 years; median, 76 years); ii) stage II, 3 patients (aged 57-71 years; median, 58 years); iii) stage III, 21 patients (aged 43-77 years; median, 61 years); and iv) stage IV, 90 patients (aged 30-84 years; median, 63 years). Patients with stage IV NSCLC (n=90) were divided into the BM group (n=26, aged 43-84 years) and non-BM group (n=64, aged 30-84 years) by clinically detectable metastatic lesions. There were no significant differences in the demographic and clinical characteristics between the BM and the non-BM group (Table I).

Landscape of somatic mutations. To delineate the somatic mutation landscape, the somatic mutations from the tumor tissue DNA of 69 patients were first analyzed by applying an NGS panel of 95 known cancer genes (Table SII). The present study mainly focused on protein-altering variants, based on the annotation of somatic SNVs and InDels. A total of 157 somatic variants of 32 mutated genes were detected in 62 out of 69 (89.86%) tumor tissues (Fig. 1A and Table SIII). To explore the feasibility of genomic profiling using peripheral blood samples, the same NGS panel was used to detect 51 plasma-derived ctDNA. In total, 77 somatic variants of 30 mutated genes were identified in 38 out of 51 (74.51%) peripheral blood samples, which was lower than that from tissue DNA (Fig. 1B and Table SIII). Furthermore, the percentages

Table I. Characteristics of patients with advanced NSCLC according to brain metastatic progression.

		Brain metastases		
Clinical characteristics	No. of patients	Yes	No	P-value
Total sample	90	26	64	0.6378
Tissue	53	14	39	
ctDNA	37	12	25	
Age, years				0.9074
≤50	18	5	13	
>50	72	21	51	
Sex				0.8135
Male	54	15	39	
Female	36	11	25	
Histology				0.999
Adenocarcinoma	80	24	56	
Squamous carcinoma	9	2	7	
Adenosquamous carcinoma	1	0	1	
Family history of lung cancer				0.999
Yes	1	0	1	
No	89	26	63	
History of pulmonary infection				0.8931
Yes	44	13	31	
No	46	13	33	
History of smoking				0.6771
Once	12	2	10	
Now	26	8	18	
Never	52	16	36	
History of alcohol consumption				0.9312
Once	8	2	6	
Now	19	6	13	
Never	63	18	45	
Pre-existing metabolic disease				0.1556
Yes	19	3	16	
No	58	20	38	
Unknown	13	3	10	
Vascular invasion				0.7495
Yes	76	23	53	
No	14	3	11	
Nerve invasion				0.5002
Yes	11	2	9	
No	79	24	55	
CYFRA21-1 at baseline				0.5084
Normal	13	6	7	
Elevated	26	9	17	
Unknown	51	11	40	
CEA at baseline				0.603
Normal	24	6	18	
Elevated	60	20	40	
Unknown	6	0	6	
NSE at baseline				0.7294
Normal	28	12	16	
Elevated	12	4	8	
Unknown	50	10	40	

Table I. Continued.

Clinical characteristics	No. of patients	Brain metastases		P-value
		Yes	No	
SCC at baseline				0.1427
Normal	24	11	13	
Elevated	12	2	10	
Unknown	54	13	41	

NSCLC, non-small cell lung cancer; ctDNA, circulating tumor DNA; CYFRA21-1, cytokeratin 19 fragment; CEA, carcinoembryonic antigen; NSE, neuron specific enolase; SCC, squamous cell carcinoma antigen.

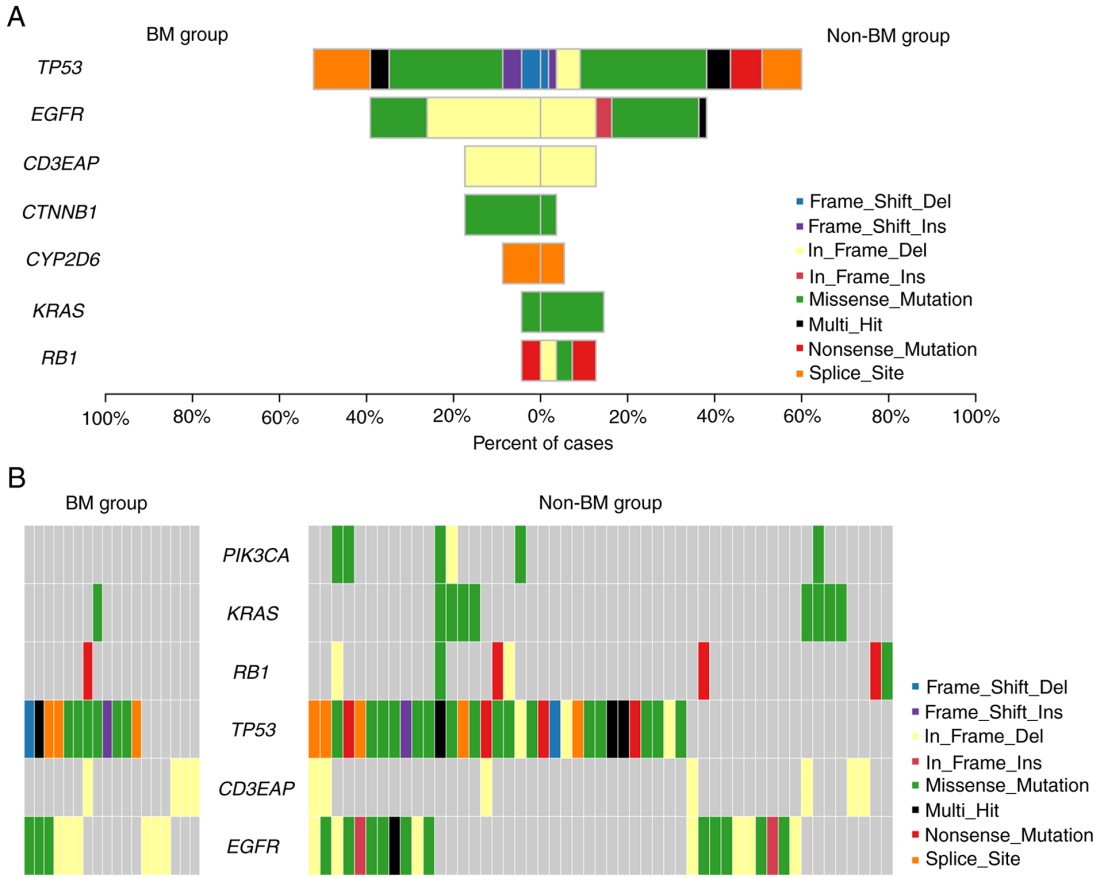

Figure 2. (A) coBarplot diagram of genomic subtyping with somatic mutations and (B) coOncoplot diagram of mutated genes in advanced NSCLC patients with (left panel) and without (right panel) BM. NSCLC, non-small cell lung cancer; BM, brain metastases.

of tissue DNA-specific mutated genes and ctDNA-specific mutated genes were 28.57% (12/42) and 23.81% (10/42), respectively, whereas the consistency rate of mutated genes was 47.62% (20/42) in NSCLC (Fig. 1C and Table SIII).

Differences in somatic mutations between the BM and non-BM group. Patients with NSCLC with BM have been shown to be significantly associated with an increased mortality rate (4). However, the underlying molecular mechanisms of the initiation and progression of BM have not yet been fully elucidated in NSCLC. In the present study, to explore this issue, the genomic characterizations of patients both from the BM and the non-BM group were first depicted using an NGS panel. In total, 47 somatic variants of 17 mutated genes were identified in 23 out of 26 (88.46%) patients with BM (Figs. 2 and S1A, and Table SIV), and 127 somatic variants of 30 mutated genes were observed in 55 of 64 (85.94%) non-BM patients (Figs. 2 and S1C, and Table SIV). To further discover the molecular differences between the BM and the non-BM group, a Venn diagram was plotted (Fig. S1B). Among the total number of 35 mutant genes, *ALK*, cytidine deaminase (*CDA*), SMAD family member 4 (*SMAD4*), superoxide dismutase 2 (*SOD2*), and Von Hippel-Lindau tumor suppressor (*VHL*) were uniquely present in the BM group, whereas 18 mutant genes [ATM serine/

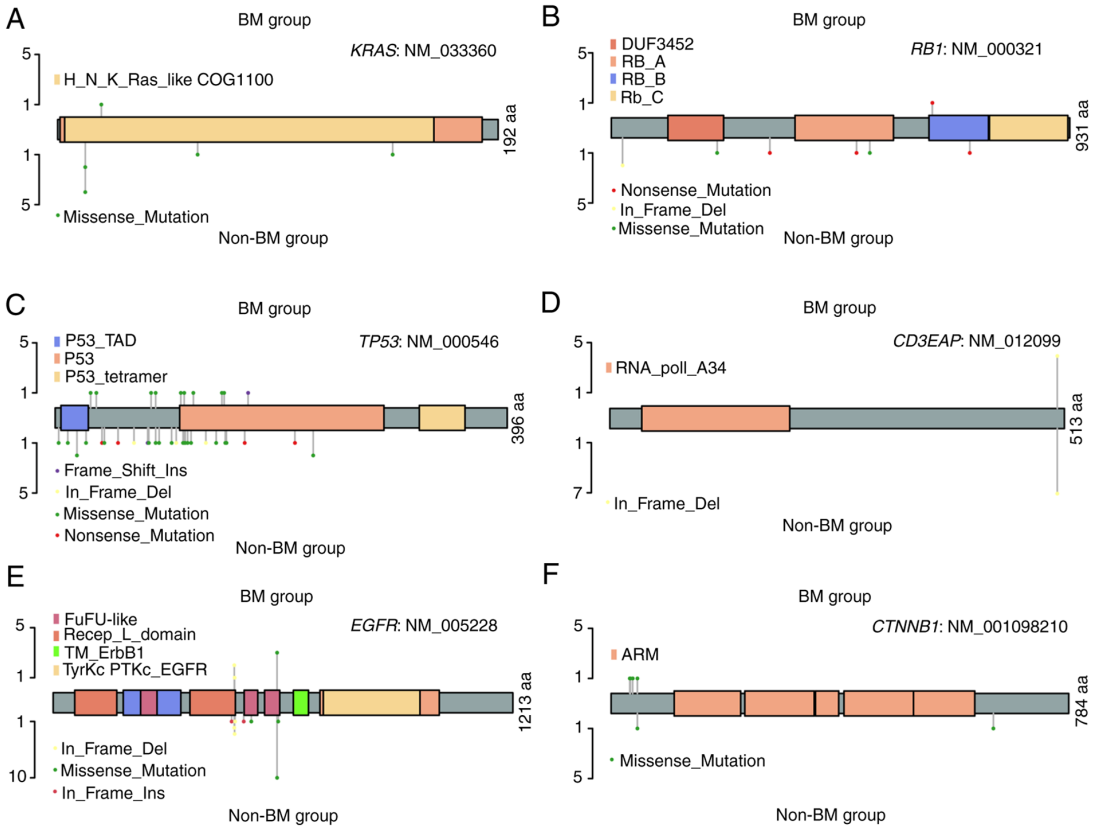

Figure 3. The protein structure and mutational proportion of (A) *KRAS*, (B) *RB1*, (C) *TP53*, (D) *CD3EAP*, (E) *EGFR*, and (F) *CTNNB1* in patients with advanced NSCLC with (top panels) and without BM (bottom panels). Protein domains are marked in different colors. Lollipops represent the locations of protein-altering variants. Square brackets indicate the proportion of patient-harbored non-synonymous mutations in each group. *CD3EAP,* DNA-directed RNA polymerase I subunit RPA34; *CTNNB1,* catenin beta-1; NSCLC, non-small cell lung cancer; BM, brain metastases.

threonine kinase (*ATM*), cyclin-dependent kinase inhibitor 2A (*CDKN2A*), Erb-B2 receptor tyrosine kinase 4 (*ERBB4*), *HRAS*, *PIK3CA*, etc.] only emerged in the non-BM group. In total, 12 mutant genes [APC regulator of WNT signaling pathway (*APC*), DNA-directed RNA polymerase I subunit RPA34 (*CD3EAP*), catenin beta-1 (*CTNNB1*), cytochrome P450 2D6 (*CYP2D6*), dihydropyrimidine dehydrogenase (*DPYD*), *EGFR*, Kirsten rat sarcoma (*KRAS*), *NRAS*, *TP53*, telomerase reverse transcriptase (*TERT*), thiopurine S-methyltransferase (*TPMT*) and RB transcriptional co-repressor 1 (*RB1*)] were concurrently present in both groups.

Moreover, the frequencies and sites of the above concurrently mutated genes were also investigated. Of note, apart from *CD3EAP*, *DPYD* and *TPMT*, the frequencies and/or sites of the concurrently mutated genes were different (Fig. 3 and Table SV). In relation to the *KRAS* gene, marked differences were observed in the mutation sites and frequencies (p.L19F vs. p.G12D, p.G12V, p.Q61H, and p.A146T, 3.85 vs. 12.5%) of these two groups (Fig. 3A and Table SV). Although about half of the patients harbored *TP53* mutations in the two groups, the types and sites of amino acid alterations were different (Fig. 3C and Table SV). The frameshift insertion of *TP53* was exclusively identified in the BM group, and in-frame deletion and nonsense mutation were only detected in the non-BM group.

Differences in somatic interactions between the BM and non-BM group. In NSCLC, patients presenting with *EGFR* mutations have a much higher incidence of BM compared to

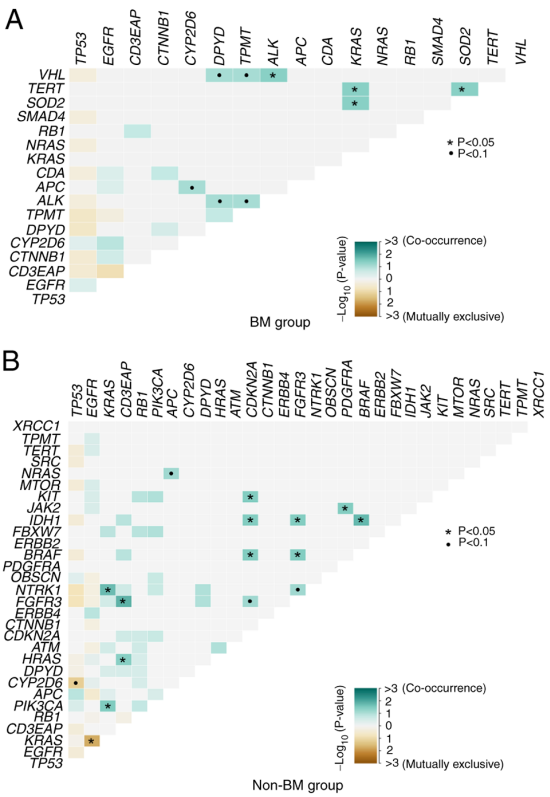

Figure 4. Spectrum of co-occurring and mutually exclusive genomic alterations in patients with advanced NSCLC (A) with and (B) without BM. NSCLC, non-small cell lung cancer; BM, brain metastases.

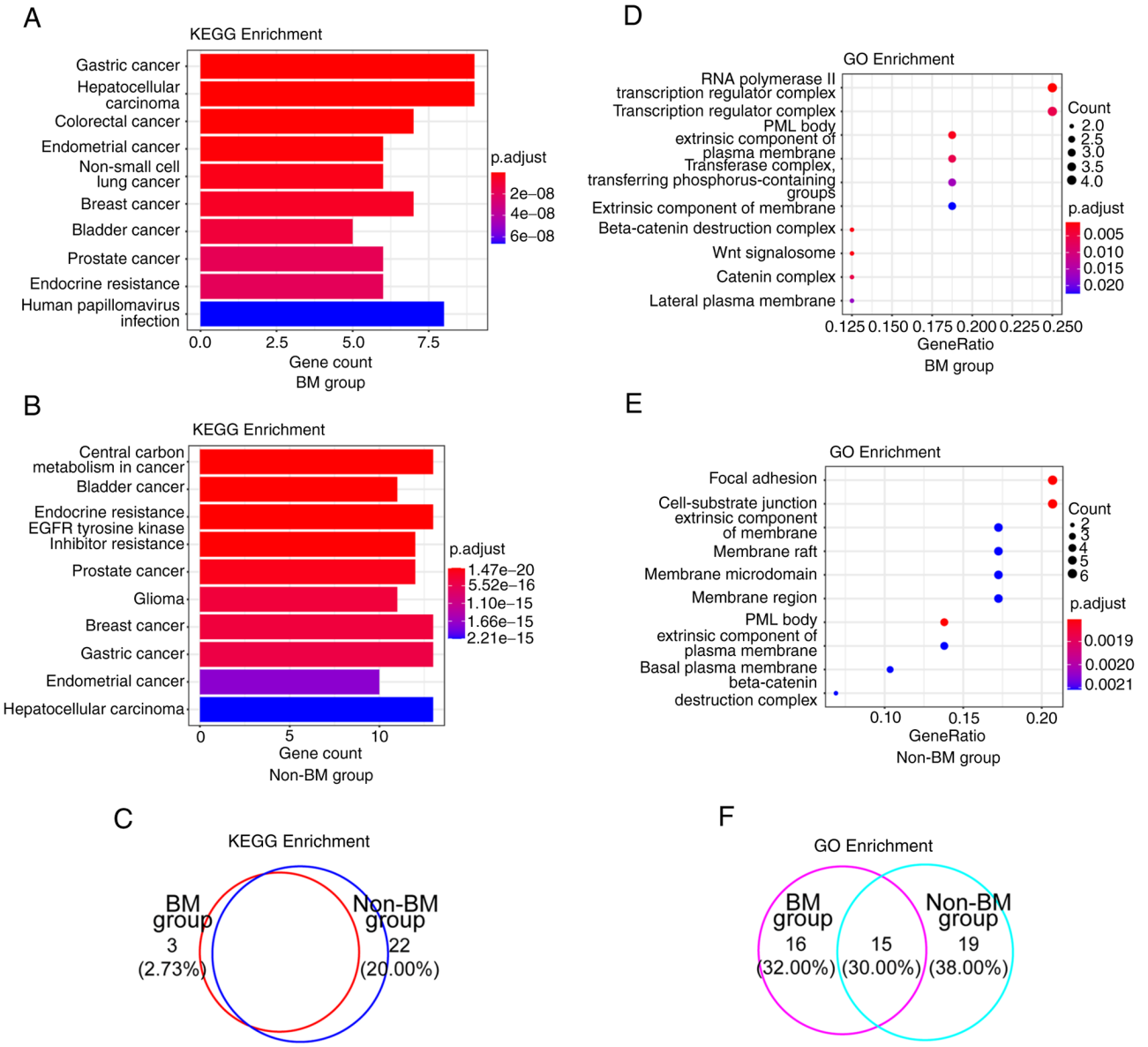

Figure 5. (A and B) Signaling pathway analysis by KEGG and (D and E) functional terms by GO enrichment analysis in patients with advanced NSCLC (A and D) with and (B and E) without BM. The value represents the number of mutated genes enriched in these functional terms. Venn diagram of (C) signaling pathways or (F) functional terms in the BM group and the non-BM group. KEGG, Kyoto Encyclopedia of Genes and Genomes; GO, Gene Ontology; NSCLC, non-small cell lung cancer; BM, brain metastases.

those without *EGFR* mutation. *EGFR* mutations and KRAS mutations are usually mutually exclusive, and *KRAS* mutations could confer resistance to EGFR-TKIs when they co-exist (32). In the present study, the somatic interactions in the BM group were different from the interactions of the non-BM group. EGFR and *KRAS* were a mutually exclusive set of genes in the non-BM group (P=0.0183) (Fig. 4B and Table SV), whereas limited mutually exclusive interactions were observed in the BM group (P=0.999) (Fig. 4A and Table SVI). Additionally, obvious differences were also detected in the co-occurring set of genes between the two groups. As demonstrated in Fig. 4, *VHL* and *ALK* (P=0.0435), *SOD2* and *KRAS* (P=0.0435), *TERT* and *KRAS* (P=0.0435), *TERT* and *SOD2* (P=0.0435) were co-occurring pair of genes in the BM group (Fig. 4A and Table SV), while *FGFR3* and *CD3EAP* (P=0.0141), isocitrate dehydrogenase [NADP(+)] 1 (*IDH1*) and *BRAF* (P=0.0182), neurotrophic receptor tyrosine kinase 1 (*NTRK1*) and *KRAS* (P=0.0189), *PIK3CA* and *KRAS* (P=0.0340), *CDKN2A* and *BRAF* (P=0.0364), and interactions between other six co-occurring pair of genes were detected in the BM group (Fig. 4B and Table SVI).

Key signaling pathways and biological functions analysis of somatic mutations in the BM and the non-BM group. In order to acquire a more incisive understanding of the biological consequences in these two groups, KEGG and GO enrichment analyses were performed. The top 10 KEGG pathways enriched by mutated genes were depicted according to gene count and P-value, and most signaling pathways were cancer-related (Fig. 5A and B, and Table II). Since patients with BM respond well to *EGFR*-TKIs, the P-value of EGFR-TKI resistance was markedly higher in the BM group, than in the non-BM group

Table II. Signaling pathways enriched by KEGG analysis in the BM group and the non-BM group.

ID	Description	Adjusted P-value	geneID
BM group			
hsa05226	Gastric cancer	1.85E-12	*TP53/TERT/KRAS/RB1/EGFR/ SMAD4/CTNNB1/ APC/NRAS*
hsa05225	Hepatocellular carcinoma	5.53E-12	*TP53/TERT/KRAS/RB1/EGFR/SMAD4/CTNNB1/ APC/NRAS*
hsa05210	Colorectal cancer	1.21E-10	*TP53/KRAS/EGFR/SMAD4/CTNNB1/APC/NRAS*
hsa05213	Endometrial cancer	7.60E-10	*TP53/KRAS/EGFR/CTNNB1/APC/NRAS*
hsa05223	Non-small cell lung cancer	2.89E-09	*TP53/KRAS/RB1/EGFR/ALK/NRAS*
hsa05224	Breast cancer	5.41E-09	*TP53/KRAS/RB1/EGFR/CTNNB1/APC/NRAS*
hsa05219	Bladder cancer	1.06E-08	*TP53/KRAS/RB1/EGFR/NRAS*
hsa05215	Prostate cancer	1.78E-08	*TP53/KRAS/RB1/EGFR/CTNNB1/NRAS*
hsa01522	Endocrine resistance	1.89E-08	*TP53/KRAS/RB1/EGFR/CYP2D6/NRAS*
hsa05165	Human papillomavirus infection	6.64E-08	*TP53/TERT/KRAS/RB1/EGFR/CTNNB1/APC/NRAS*
Non-BM group			
hsa05230	Central carbon metabolism in cancer	1.47E-20	*PDGFRA/NRAS/TP53/PIK3CA/KRAS/EGFR/HR AS/MTOR/KIT/FGFR3/NTRK1/IDH1/ERBB2*
hsa05219	Bladder cancer	2.47E-19	*NRAS/TP53/RB1/KRAS/EGFR/HRAS/CDKN2A/ FGFR3/SRC/BRAF/ERBB2*
hsa01522	Endocrine resistance	1.58E-18	*CYP2D6/NRAS/TP53/PIK3CA/RB1/KRAS/EGFR/ HRAS/CDKN2A/MTOR/SRC/BRAF/ERBB2*
hsa01521	EGFR tyrosine kinase inhibitor resistance	7.84E-18	*PDGFRA/NRAS/PIK3CA/KRAS/ EGFR/HRAS/ JAK2/MTOR/FGFR3/ SRC/BRAF/ERBB2*
hsa05215	Prostate cancer	1.06E-16	*PDGFRA/NRAS/TP53/PIK3CA/RB1/ KRAS/EGFR/ HRAS/CTNNB1/MTOR/BRAF/ERBB2*
hsa05214	Glioma	3.59E-16	*PDGFRA/NRAS/TP53/PIK3CA/RB1/KRAS/EGFR/ HRAS/CDKN2A/MTOR/BRAF*
hsa05224	Breast cancer	3.76E-16	*NRAS/TP53/PIK3CA/RB1/KRAS/EGFR/HRAS/ CTNNB1/APC/MTOR/ KIT/BRAF/ERBB2*
hsa05226	Gastric cancer	4.50E-16	*NRAS/TP53/PIK3CA/RB1/KRAS/EGFR/HRAS/ CTNNB1/APC/MTOR/ BRAF/TERT/ERBB2*
hsa05213	Endometrial cancer	1.77E-15	*NRAS/TP53/PIK3CA/KRAS/EGFR/HRAS/CTNNB1/ APC/BRAF/ERBB2*
hsa05225	Hepatocellular carcinoma	2.21E-15	*NRAS/TP53/PIK3CA/RB1/KRAS/EGFR/HRAS/ CDKN2A/CTNNB1/APC/ MTOR/BRAF/TERT*

(4.50E-04 vs. 7.84E-18) (Tables II and SVII). In GO enrichment analysis, functional categories were most involved in RNA polymerase II transcription regulator complex in the BM group (Fig. 5D and Table III) and promyelocytic leukemia nuclear body in the non-BM group (Fig. 5E and Table III). Furthermore, five mutated genes uniquely present in the BM group were prevailingly distributed in transcription regulator complex, RNA polymerase complex, bicellular tight junction, tight junction, apical junction complex, and so forth (Tables III and SVII). Collectively, a high consistency of altered signaling pathways between these two groups according to KEGG analysis was observed (Fig. 5C), whereas the percentage was decreased in GO analysis-related altered functional terms [Fig. 5F; KEGG analysis, 77.27% (85/110) vs. GO analysis, 30.00% (15/50)].

Clinical actionability for the therapy of targeted agents. In order to evaluate the clinical utility of anticipative molecular profiling, all mutations were divided into different levels, according to the evidence of clinical actionability in OncoKB (Fig. 6A). As standard therapeutic biomarkers, a cluster of gene mutations was approved by the FDA. In the present cohort, 47 out of 120 (39.17%) patients possessed at least one actionable alteration. Among the patients with stage IV disease, level_1 accounted for 34.44% (31/90), including missense mutations of *BRAF*, *EGFR*, *IDH1*, *PDGFRA* and *PIK3CA*, a nonsense mutation of *ATM* and an in-frame insertion of *EGFR*; level_2 accounted for 4.44% (4/90), including missense mutations of *NRAS* and *PIK3CA* and an in-frame deletion of *PIK3CA*; level_3 accounted for 1.11% (1/90), including an in-frame

Table III. Functional terms enriched by GO enrichment analysis in the BM and the non-BM group.

ID	Description	Adjusted P-value	geneID
BM group			
GO:0090575	RNA polymerase II transcription regulator complex	0.0010	*TP53/RB1/SMAD4/CTNNB1*
GO:0030877	Beta-catenin destruction complex	0.0017	*CTNNB1/APC*
GO:1990909	Wnt signalosome	0.0017	*CTNNB1/APC*
GO:0016605	PML body	0.0023	*TP53/TERT/RB1*
GO:0016342	Catenin complex	0.0060	*CTNNB1/APC*
GO:0005667	Transcription regulator complex	0.0060	*TP53/RB1/SMAD4/ CTNNB1*
GO:0019897	Extrinsic component of plasma membrane	0.0060	*KRAS/CTNNB1/APC*
GO:0061695	Transferase complex, transferring phosphorus-containing groups	0.0163	*TP53/TERT/RB1*
GO:0016328	Lateral plasma membrane	0.0173	*CTNNB1/APC*
GO:0019898	Extrinsic component of membrane	0.0225	*KRAS/CTNNB1/APC*
Non-BM group			
GO:0016605	PML body	0.0018	*TP53/RB1/MTOR/TERT*
GO:0005925	Focal adhesion	0.0018	*KRAS/EGFR/JAK2/CTNNB1/ FGFR3/SRC*
GO:0030055	Cell-substrate junction	0.0018	*KRAS/EGFR/JAK2/ CTNNB1/ FGFR3/SRC*
GO:0009925	Basal plasma membrane	0.0021	*ERBB4/EGFR/ERBB2*
GO:0019898	Extrinsic component of membrane	0.0021	*PIK3CA/KRAS/CTNNB1/APC/SRC*
GO:0045121	Membrane raft	0.0021	*KRAS/EGFR/JAK2/CTNNB1/SRC*
GO:0098857	Membrane microdomain	0.0021	*KRAS/EGFR/JAK2/ CTNNB1/SRC*
GO:0019897	Extrinsic component of plasma membrane	0.0021	*KRAS/CTNNB1/APC/SRC*
GO:0098589	Membrane region	0.0021	*KRAS/EGFR/JAK2/CTNNB1/SRC*
GO:0030877	Beta-catenin destruction complex	0.0021	*CTNNB1/APC*

insertion of *EGFR*; level_4 accounted for 1.11% (1/90), including missense mutations of *CDKN2A* (Fig. 6B, E and H, and Table SVIII). Additionally, it was also observed that non-BM patients had a slightly higher percentage of actionable alterations than patients with BM, namely 45.31% (29/64) vs. 30.77% (8/26) (Fig. 6D, F, G, I, J, and Table SVIII).

ctDNA analysis has a higher consistency of genomic profiling in the non-BM group as compared with that in the BM group. To compare the feasibility of genomic profiling of advanced patients with or without BM using plasma-derived ctDNA, somatic mutations from 14 tumor tissues and 12 peripheral blood samples were analyzed in the BM group by the above NGS panel. A total of 32 somatic variants of 12 mutated genes were identified in 13 out of 14 (92.86%) tumor tissue DNA samples (Fig. 7A and Table SIX), and 15 somatic variants of 10 mutant genes were detected in 10 of 12 (83.33%) plasma-derived ctDNA (Fig. 7B and Table SIX). Meanwhile, eighty-three somatic variants of 22 mutated genes in 36 of 39 (92.31%) tumor tissue DNA were also detected (Fig. 7C and Table SX), as well as 44 somatic variants of 21 mutated genes in 19 out of 25 (76.00%) plasma-derived ctDNA (Fig. 7D and Table SX) in the non-BM group. In summary, 43.33% (13/30) of the mutated genes were detected by both tumor tissue DNA analysis and ctDNA analysis in the non-BM group (Fig. 7E), whereas the percentage was only 29.41% (5/17) in the BM group (Fig. 7E).

Discussion

Exploring the genomic alterations is crucial for clinical management in NSCLC patients with BM. Although dynamic mutation landscapes have been reported, systematic comparisons of genomic characteristics between the BM and the non-BM groups remain limited. In the present study, 174 somatic mutations of 35 mutated genes were identified in 90 patients with stage IV NSCLC using an NGS panel of 95 known cancer genes. Significant differences between the BM and the non-BM group were detected in somatic mutations, somatic interactions, key signaling pathways, functional biological information and clinical actionability for the therapy of targeted agents. Finally, it was also observed that ctDNA analysis presented with a higher consistency for genomic profiling of the non-BM than that of the BM group, indicating that ctDNA analysis may serve as a more credible alternative for genomic profiling in advanced NSCLC patients without BM.

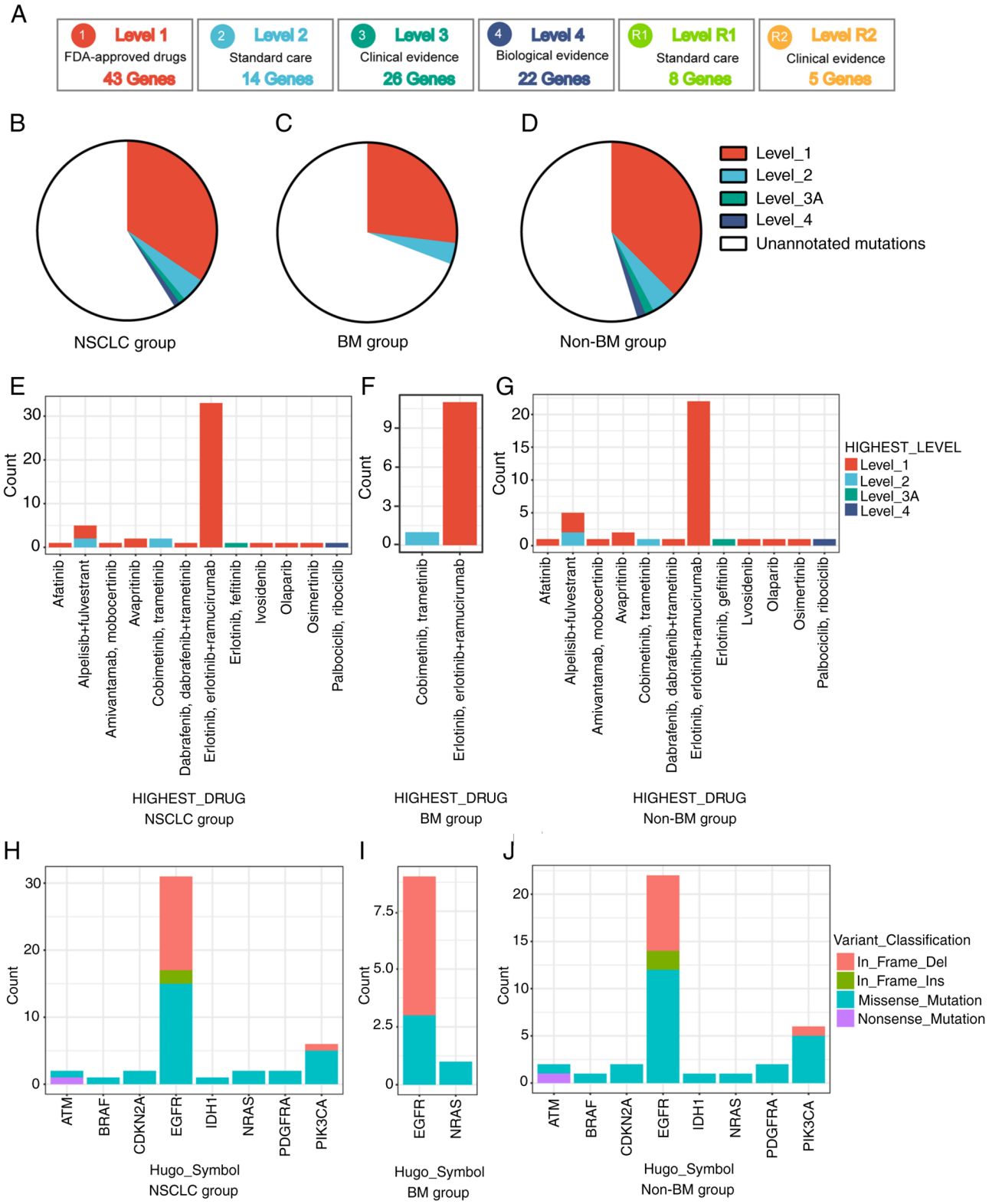

Figure 6. (A) The clinical actionability of somatic mutations annotated according to OncoKB. The highest level of actionable alterations in (B) patients with advanced NSCLC (n=90), (C) the BM group (n=26), and (D) the non-BM group (n=64). Distribution of actionable alterations in (E) patients with advanced NSCLC, (F) the BM group, and (G) the non-BM group. Distribution of alteration types in (H) patients with advanced NSCLC, (I) the BM group, and (J) the non-BM group. NSCLC, non-small cell lung cancer; BM, brain metastases.

In the present study, 17 mutated genes and 30 mutated genes were identified in the BM and the non-BM group, respectively. Among these genes, five genes, including *ALK*, *CDA*, *SMAD4*, *SOD2* and *VHL* were uniquely present in patients with BM. *ALK* is a tyrosine kinase and its constitutively activated mutation renders *ALK* a formidable cancer driver gene (33,34). BM occurs frequently in tumors harboring *ALK* rearrangements (10), and its clinical significance has been considered

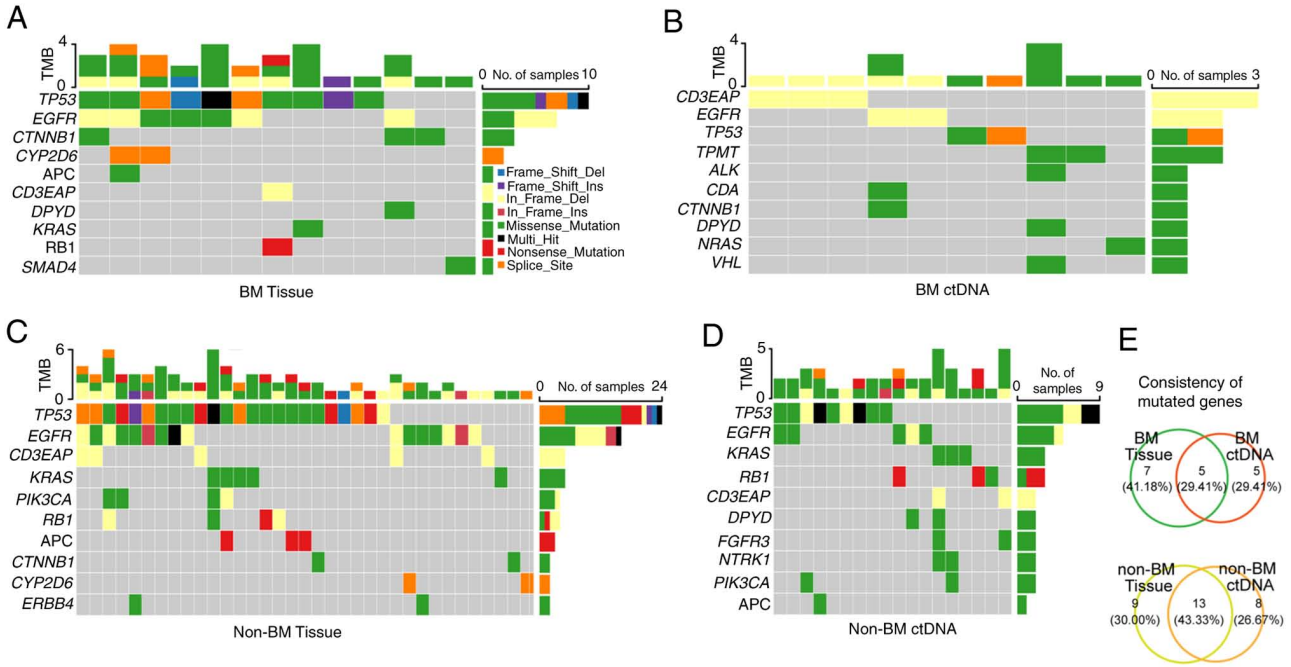

Figure 7. Somatic mutation landscapes of patients with advanced NSCLC with (A and B) or without (C and D) BM from (A and C) tumor tissue DNA and (B and D) ctDNA. (E) Venn diagrams of mutated genes derived from tumor tissue DNA analysis and ctDNA analysis in the (top panel) BM group and (bottom panel) the non-BM group.

to be critical. Several *ALK* inhibitors have been reported to demonstrate conspicuous activity in brain metastatic patients with crizotinib-resistant *ALK*-positive NSCLC, including second-generation (brigatinib and alectinib) (35-37), and third-generation therapeutics (lorlatinib) (38,39). Additionally, *ALK* and *VHL* (P=0.0435) are exclusively co-occurring genes in the BM group, which was reported in Chinese patients with NSCLC for the first time, to the best of our knowledge. More notably, as the first generation of the blood-brain barrier (BBB)-penetrating TKIs, AZD3759 can activate a p53-*SMAD4* positive feedback loop and lead to apoptosis in hepatoma cells (40), offering a promising future approach for the treatment of brain metastatic NSCLC patients by AZD3759 (41). Collectively, the data of the present study may contribute to an improved comprehension of the underlying molecular mechanisms of patients with NSCLC with BM and may provide prospective therapeutic targets for this specific subgroup.

Additionally, five genes exclusively identified in the BM group were distributed in the Hippo signaling pathway, pyrimidine metabolism (PyM), and pantothenate and CoA biosynthesis, according to KEGG enrichment analyses. As a key mediator in the Hippo signaling pathway, Yes-associated protein (YAP) has been founded to facilitate drug resistance and tumorigenesis in NSCLC (42-45). Furthermore, YAP has been reported to play a crucial role for the promotion of BM in lung adenocarcinoma patients, and the inhibition of YAP by shRNA may significantly suppress migration and invasion abilities of metastatic NSCLC cell lines H2030-BrM3 in a murine model (46). Combined with the current results, these findings may provide prospective therapeutic approaches by modulating the members or mediators of the Hippo signaling pathway in brain metastatic patients with NSCLC. As a complex enzymatic network, the main function of PyM is to integrate *de novo* nucleotide synthesis, nucleoside salvage, and catalytic degradation of pyrimidines. In cancer cells, the *de novo* nucleotide synthesis pathway continuously provides deoxyribonucleoside triphosphates (dNTPs) to sustain uncontrolled proliferation, being different from normal cell *de novo* nucleotide synthesis (47,48). Until recently, PyM has been mainly implicated in the differentiation of leukemic cells; however, little is known about its roles in the differentiation of solid tumors (49). To the best of our knowledge, the present finding is the first report on PyM as an exclusive signaling pathway in Chinese patients with NSCLC with BM. However, further studies are required in order to discern whether PyM signaling pathway plays a critical role in the initiation and/or progression of BM in NSCLC.

More importantly, it was also demonstrated that ctDNA analysis is more feasible as an alternative for somatic mutation landscapes of non-BM patients than that of BM patients by the higher consistency between ctDNA analysis and tumor DNA analysis (43.33 vs. 29.41%). A possible explanation for the discrepancies between ctDNA analysis and tumor DNA analysis may be the inhibition of tumor cell release into the bloodstream by the BBB in patients with BM (50,51). Thus, the basic detection rate of genomic alterations derived from peripheral blood ctDNA in the BM group has been reported to be lower than that in the non-BM group (52,53). In a similar study, Aldea *et al* (53) demonstrated that ctDNA was positive in 52% of isolated central nervous system progression (iCNS) vs. 84% in extra-CNS only (noCNS), which was accompanied by a lower detection rate of pathogenic driver mutations (37 vs. 77%) and resistance alterations (6 vs. 45%). However, it cannot be overlooked that liquid biopsy is a potent method with which to improve the identification of actionable biomarkers when tumor tissue is unavailable (52,54,55). In the present study,

plasma-derived ctDNA analysis improved the detection rate of *EGFR* actionable mutations by a 15.39% (4/26) increase in the BM group, and four patients had the opportunity to receive targeted therapies (erlotinib/erlotinib + ramucirumab/afatinib/gefitinib/osimertinib/dacomitinib) and/or participate in clinical trials. Consequently, the data of the present study are consistent with those of previous studies in which the identification of actionable mutations is growing in advanced NSCLC patients with the aid of plasma-derived ctDNA (56,57).

In the present study, one of the main limitations is that NGS data were obtained from tumor tissue DNA or plasma-derived ctDNA without the simultaneous analysis of matched normal tissue to delete the germline mutations. Thus, for a single sample the analysis was not complete; however, it may be considered adequate for the acquisition of actionable genomic alterations for the application of guided clinical treatment based on the suitable filter conditions (please see the 'Materials and methods' section, 'Bioinformatics analysis') (30,58-65). However, it cannot be disregarded that either multiregional biopsies or more than one type of biopsies may be costlier than the analysis of a single tumor sample without the inclusion of matched normal tissue. Another main limitation is the absence of a genomic profile, derived from brain tumor tissue DNA due to difficulties in the acquisition of brain tissue samples from NSCLC patients with BM. Additionally, although all patients were recruited for a prospective study, the collection of NGS data was retrospective. Lastly, further multiple-institution research with larger sample sizes is required to validate the present conclusions.

In conclusion, the somatic mutation landscapes of NSCLC with and without BM were compared, and significant differences in somatic mutations, somatic interactions, key signaling pathways, functional biological information, and clinical actionability for the therapy of targeted agents were observed between the BM group and the non-BM group. Moreover, plasma-derived ctDNA analysis may be a more reliable alternative for genomic profiling of advanced patients without BM, based on the higher consistency between ctDNA analysis and tumor DNA analysis in NSCLC.

Acknowledgements

Not applicable.

Funding

No funding was received.

Availability of data and materials

The datasets generated and/or analyzed during the current study are available from the corresponding author on reasonable request. The next generation sequencing data are available at the NCBI BioProject database (Reference no. PRJNA759391; https://www.ncbi.nlm.nih.gov/bioproject/PRJNA759391).

Authors' contributions

RN, JZ, JL and WL conceptualized and designed the present study. RN, HZ, JM, PL, SW and JZ were involved in the acquisition of samples. YW and SW performed the high-throughput sequencing experiments. YW, HJ, WH and LJ performed the bioinformatics analysis. HJ, WH, YX and LJ were involved in the statistical analysis. RN, HJ, LJ, YW, JZ and WL were responsible for administrative/technical/material support and study supervision. HJ and JL wrote the manuscript. RN, HJ, WH, HZ, JM, PL, LJ, YX, SW, and JL critically revised the article. All authors have read and approved the final manuscript. LJ and WL confirm the authenticity of all the raw data.

Ethics approval and consent to participate

The part of this study involving human participants was reviewed and approved by the Medical Ethics Committee of Affiliated 3201 Hospital of Xi'an Jiaotong University [No.008(2017)]. Written informed consent was obtained from all participants involved in the present study, according to national legislation and institutional requirements.

Patient consent for publication

The publication of data was approved by all patients.

Competing interests

The authors declare that they have no competing interests.

References

1. Schuette W: Treatment of brain metastases from lung cancer: Chemotherapy. Lung Cancer 45 (Suppl 2): S253-S257, 2004.
2. Khalifa J, Amini A, Popat S, Gaspar LE and Faivre-Finn C; International Association for the Study of Lung Cancer Advanced Radiation Technology C: Brain metastases from NSCLC: Radiation therapy in the Era of targeted therapies. J Thorac Oncol 11: 1627-1643, 2016.
3. Langer CJ and Mehta MP: Current management of brain metastases, with a focus on systemic options. J Clin Oncol 23: 6207-6219, 2005.
4. Owen S and Souhami L: The management of brain metastases in non-small cell lung cancer. Front Oncol 4: 248, 2014.
5. D'Antonio C, Passaro A, Gori B, Del Signore E, Migliorino MR, Ricciardi S, Fulvi A and de Marinis F: Bone and brain metastasis in lung cancer: Recent advances in therapeutic strategies. Ther Adv Med Oncol 6: 101-114, 2014.
6. Lagerwaard FJ, Levendag PC, Nowak PJ, Eijkenboom WM, Hanssens PE and Schmitz PI: Identification of prognostic factors in patients with brain metastases: A review of 1292 patients. Int J Radiat Oncol Biol Phys 43: 795-803, 1999.
7. Shi AA, Digumarthy SR, Temel JS, Halpern EF, Kuester LB and Aquino SL: Does initial staging or tumor histology better identify asymptomatic brain metastases in patients with non-small cell lung cancer? J Thorac Oncol 1: 205-210, 2006.
8. Mujoomdar A, Austin JH, Malhotra R, Powell CA, Pearson GD, Shiau MC and Raftopoulos H: Clinical predictors of metastatic disease to the brain from non-small cell lung carcinoma: Primary tumor size, cell type, and lymph node metastases. Radiology 242: 882-888, 2007.
9. Shin DY, Na II, Kim CH, Park S, Baek H and Yang SH: EGFR mutation and brain metastasis in pulmonary adenocarcinomas. J Thorac Oncol 9: 195-199, 2014.
10. Fallet V, Cadranel J, Doubre H, Toper C, Monnet I, Chinet T, Oliviero G, Foulon G, De Cremoux H, Vieira T, *et al*: Prospective screening for ALK: Clinical features and outcome according to ALK status. Eur J Cancer 50: 1239-1246, 2014.
11. Heigener DF, Kerr KM, Laing GM, Mok TSK, Moiseyenko FV and Reck M: Redefining treatment paradigms in first-line advanced non-small-cell lung cancer. Clin Cancer Res 25: 4881-4887, 2019.

12. Lynch TJ, Bell DW, Sordella R, Gurubhagavatula S, Okimoto RA, Brannigan BW, Harris PL, Haserlat SM, Supko JG, Haluska FG, *et al*: Activating mutations in the epidermal growth factor receptor underlying responsiveness of non-small-cell lung cancer to gefitinib. N Engl J Med 350: 2129-2139, 2004.
13. Brastianos PK, Carter SL, Santagata S, Cahill DP, Taylor-Weiner A, Jones RT, Van Allen EM, Lawrence MS, Horowitz PM, Cibulskis K, *et al*: Genomic characterization of brain metastases reveals branched evolution and potential therapeutic targets. Cancer Discov 5: 1164-1177, 2015.
14. Shih DJH, Nayyar N, Bihun I, Dagogo-Jack I, Gill CM, Aquilanti E, Bertalan M, Kaplan A, D'Andrea MR, Chukwueke U, *et al*: Genomic characterization of human brain metastases identifies drivers of metastatic lung adenocarcinoma. Nat Genet 52: 371-377, 2020.
15. Fernandes Marques J, Pereira Reis J, Fernandes G, Hespanhol V, Machado JC and Costa JL: Circulating tumor DNA: A step into the future of cancer management. Acta Cytol 63: 456-465, 2019.
16. Jahr S, Hentze H, Englisch S, Hardt D, Fackelmayer FO, Hesch RD and Knippers R: DNA fragments in the blood plasma of cancer patients: Quantitations and evidence for their origin from apoptotic and necrotic cells. Cancer Res 61: 1659-1665, 2001.
17. Wan JCM, Massie C, Garcia-Corbacho J, Mouliere F, Brenton JD, Caldas C, Pacey S, Baird R and Rosenfeld N: Liquid biopsies come of age: Towards implementation of circulating tumour DNA. Nat Rev Cancer 17: 223-238, 2017.
18. Keller L and Pantel K: Unravelling tumour heterogeneity by single-cell profiling of circulating tumour cells. Nat Rev Cancer 19: 553-567, 2019.
19. Gerlinger M, Rowan AJ, Horswell S, Math M, Larkin J, Endesfelder D, Gronroos E, Martinez P, Matthews N, Stewart A, *et al*: Intratumor heterogeneity and branched evolution revealed by multiregion sequencing. N Engl J Med 366: 883-892, 2012.
20. Murtaza M, Dawson SJ, Pogrebniak K, Rueda OM, Provenzano E, Grant J, Chin SF, Tsui DWY, Marass F, Gale D, *et al*: Multifocal clonal evolution characterized using circulating tumour DNA in a case of metastatic breast cancer. Nat Commun 6: 8760, 2015.
21. Marusyk A, Janiszewska M and Polyak K: Intratumor heterogeneity: The Rosetta stone of therapy resistance. Cancer Cell 37: 471-484, 2020.
22. Rolfo C, Mack PC, Scagliotti GV, Baas P, Barlesi F, Bivona TG, Herbst RS, Mok TS, Peled N, Pirker R, *et al*: Liquid biopsy for advanced non-small cell lung cancer (NSCLC): A statement paper from the IASLC. J Thorac Oncol 13: 1248-1268, 2018.
23. Chen G, Cai Z, Li Z, Dong X, Xu H, Lin J, Chen L, Zhang H, Liu X and Liu J: Clonal evolution in long-term follow-up patients with hepatocellular carcinoma. Int J Cancer 143: 2862-2870, 2018.
24. Travis WD, Brambilla E, Nicholson AG, Yatabe Y, Austin JHM, Beasley MB, Chirieac LR, Dacic S, Duhig E, Flieder DB, *et al*: The 2015 World health organization classification of lung tumors: Impact of genetic, clinical and radiologic advances since the 2004 classification. J Thorac Oncol 10: 1243-1260, 2015.
25. Gandevia B and Tovell A: Declaration of Helsinki. Med J Aust 2: 320-321, 1964.
26. Li H and Durbin R: Fast and accurate long-read alignment with Burrows-Wheeler transform. Bioinformatics 26: 589-595, 2010.
27. Lai Z, Markovets A, Ahdesmaki M, Chapman B, Hofmann O, McEwen R, Johnson J, Dougherty B, Barrett JC and Dry JR: VarDict: A novel and versatile variant caller for next-generation sequencing in cancer research. Nucleic Acids Res 44: e108, 2016.
28. Wang K, Li M and Hakonarson H: ANNOVAR: functional annotation of genetic variants from high-throughput sequencing data. Nucleic Acids Res 38: e164, 2010.
29. Adzhubei IA, Schmidt S, Peshkin L, Ramensky VE, Gerasimova A, Bork P, Kondrashov AS and Sunyaev SR: A method and server for predicting damaging missense mutations. Nat Methods 7: 248-249, 2010.
30. Schwarz JM, Rodelsperger C, Schuelke M and Seelow D: MutationTaster evaluates disease-causing potential of sequence alterations. Nat Methods 7: 575-576, 2010.
31. Yu G, Wang LG, Han Y and He QY: clusterProfiler: An R package for comparing biological themes among gene clusters. OMICS 16: 284-287, 2012.
32. Pao W, Wang TY, Riely GJ, Miller VA, Pan Q, Ladanyi M, Zakowski MF, Heelan RT, Kris MG and Varmus HE: KRAS mutations and primary resistance of lung adenocarcinomas to gefitinib or erlotinib. PLoS Med 2: e17, 2005.
33. Lin JJ, Riely GJ and Shaw AT: Targeting ALK: Precision medicine takes on drug resistance. Cancer Discov 7: 137-155, 2017.
34. Holla VR, Elamin YY, Bailey AM, Johnson AM, Litzenburger BC, Khotskaya YB, Sanchez NS, Zeng J, Shufean MA, Shaw KR, *et al*: ALK: A tyrosine kinase target for cancer therapy. Cold Spring Harb Mol Case Stud 3: a001115, 2017.
35. Camidge DR, Kim DW, Tiseo M, Langer CJ, Ahn MJ, Shaw AT, Huber RM, Hochmair MJ, Lee DH, Bazhenova LA, *et al*: Exploratory analysis of brigatinib activity in patients with anaplastic lymphoma kinase-positive non-small-cell lung cancer and brain metastases in two clinical trials. J Clin Oncol 36: 2693-2701, 2018.
36. Gadgeel SM, Gandhi L, Riely GJ, Chiappori AA, West HL, Azada MC, Morcos PN, Lee RM, Garcia L, Yu L, *et al*: Safety and activity of alectinib against systemic disease and brain metastases in patients with crizotinib-resistant ALK-rearranged non-small-cell lung cancer (AF-002JG): Results from the dose-finding portion of a phase 1/2 study. Lancet Oncol 15: 1119-1128, 2014.
37. Tomasini P, Egea J, Souquet-Bressand M, Greillier L and Barlesi F: Alectinib in the treatment of ALK-positive metastatic non-small cell lung cancer: Clinical trial evidence and experience with a focus on brain metastases. Ther Adv Respir Dis: Feb 21, 2019 (Epub ahead of print).
38. Solomon BJ, Besse B, Bauer TM, Felip E, Soo RA, Camidge DR, Chiari R, Bearz A, Lin CC, Gadgeel SM, *et al*: Lorlatinib in patients with ALK-positive non-small-cell lung cancer: Results from a global phase 2 study. Lancet Oncol 19: 1654-1667, 2018.
39. Naito T, Shiraishi H and Fujiwara Y: Brigatinib and lorlatinib: Their effect on ALK inhibitors in NSCLC focusing on resistant mutations and central nervous system metastases. Jpn J Clin Oncol 51: 37-44, 2021.
40. Chao D, Pang L, Shi Y, Wang W and Liu K: AZD3759 induces apoptosis in hepatoma cells by activating a p53-SMAD4 positive feedback loop. Biochem Biophys Res Commun 509: 535-540, 2019.
41. Hochmair M: Medical treatment options for patients with epidermal growth factor receptor mutation-positive non-small cell lung cancer suffering from brain metastases and/or leptomeningeal disease. Target Oncol 13: 269-285, 2018.
42. Lorenzetto E, Brenca M, Boeri M, Verri C, Piccinin E, Gasparini P, Facchinetti F, Rossi S, Salvatore G, Massimino M, *et al*: YAP1 acts as oncogenic target of 11q22 amplification in multiple cancer subtypes. Oncotarget 5: 2608-2621, 2014.
43. You B, Yang YL, Xu Z, Dai Y, Liu S, Mao JH, Tetsu O, Li H, Jablons DM and You L: Inhibition of ERK1/2 down-regulates the Hippo/YAP signaling pathway in human NSCLC cells. Oncotarget 6: 4357-4368, 2015.
44. Cheng H, Zhang Z, Rodriguez-Barrueco R, Borczuk A, Liu H, Yu J, Silva JM, Cheng SK, Perez-Soler R and Halmos B: Functional genomics screen identifies YAP1 as a key determinant to enhance treatment sensitivity in lung cancer cells. Oncotarget 7: 28976-28988, 2016.
45. Hsu PC, You B, Yang YL, Zhang WQ, Wang YC, Xu Z, Dai Y, Liu S, Yang CT, Li H, *et al*: YAP promotes erlotinib resistance in human non-small cell lung cancer cells. Oncotarget 7: 51922-51933, 2016.
46. Hsu PC, Miao J, Huang Z, Yang YL, Xu Z, You J, Dai Y, Yeh CC, Chan G, Liu S, *et al*: Inhibition of yes-associated protein suppresses brain metastasis of human lung adenocarcinoma in a murine model. J Cell Mol Med 22: 3073-3085, 2018.
47. Villa E, Ali ES, Sahu U and Ben-Sahra I: Cancer cells tune the signaling pathways to empower de novo synthesis of nucleotides. Cancers (Basel) 11: 688, 2019.
48. Buj R and Aird KM: Deoxyribonucleotide triphosphate metabolism in cancer and metabolic disease. Front Endocrinol (Lausanne) 9: 177, 2018.
49. Shiotani T, Hashimoto Y, Fujita J, Yamauchi N, Yamaji Y, Futami H, Bungo M, Nakamura H, Tanaka T and Irino S: Reversal of enzymic phenotype of thymidine metabolism in induced differentiation of U-937 cells. Cancer Res 49: 6758-6763, 1989.
50. Hanssen A, Riebensahm C, Mohme M, Joosse SA, Velthaus JL, Berger LA, Bernreuther C, Glatzel M, Loges S, Lamszus K, *et al*: Frequency of circulating tumor cells (CTC) in patients with brain metastases: Implications as a risk assessment marker in oligo-metastatic disease. Cancers (Basel) 10: 527, 2018.

51. Riebensahm C, Joosse SA, Mohme M, Hanssen A, Matschke J, Goy Y, Witzel I, Lamszus K, Kropidlowski J, Petersen C, *et al*: Clonality of circulating tumor cells in breast cancer brain metastasis patients. Breast Cancer Res 21: 101, 2019.
52. Ye Y, Luo Z and Shi D: Use of cell free DNA as a prognostic biomarker in non-small cell lung cancer patients with bone metastasis. Int J Biol Markers 34: 381-388, 2019.
53. Aldea M, Hendriks L, Mezquita L, Jovelet C, Planchard D, Auclin E, Remon J, Howarth K, Benitez JC, Gazzah A, *et al*: Circulating tumor DNA analysis for patients with oncogene-addicted NSCLC with isolated central nervous system progression. J Thorac Oncol 15: 383-391, 2020.
54. Gedvilaite V, Schveigert D and Cicenas S: Cell-free DNA in non-small cell lung cancer. Acta Med Litu 24: 138-144, 2017.
55. Nygaard AD, Garm Spindler KL, Pallisgaard N, Andersen RF and Jakobsen A: The prognostic value of KRAS mutated plasma DNA in advanced non-small cell lung cancer. Lung Cancer 79: 312-317, 2013.
56. Aggarwal C, Thompson JC, Black TA, Katz SI, Fan R, Yee SS, Chien AL, Evans TL, Bauml JM, Alley EW, *et al*: Clinical implications of plasma-based genotyping with the delivery of personalized therapy in metastatic non-small cell lung cancer. JAMA Oncol 5: 173-180, 2019.
57. Mack PC, Banks KC, Espenschied CR, Burich RA, Zill OA, Lee CE, Riess JW, Mortimer SA, Talasaz A, Lanman RB and Gandara DR: Spectrum of driver mutations and clinical impact of circulating tumor DNA analysis in non-small cell lung cancer: Analysis of over 8000 cases. Cancer 126: 3219-3228, 2020.
58. Adzhubei I, Jordan DM and Sunyaev SR: Predicting functional effect of human missense mutations using PolyPhen-2. Curr Protoc Hum Genet Chapter 7: Unit7 20, 2013.
59. 1000 Genomes Project Consortium; Auton A, Brooks LD, Durbin RM, Garrison EP, Kang HM, Korbel JO, Marchini JL, McCarthy S, McVean GA and Abecasis GR: A global reference for human genetic variation. Nature 526: 68-74, 2015.
60. Kircher M, Witten DM, Jain P, O'Roak BJ, Cooper GM and Shendure J: A general framework for estimating the relative pathogenicity of human genetic variants. Nat Genet 46: 310-315, 2014.
61. Ng PC and Henikoff S: SIFT: Predicting amino acid changes that affect protein function. Nucleic Acids Res 31: 3812-3814, 2003.
62. McNulty SN, Parikh BA, Duncavage EJ, Heusel JW and Pfeifer JD: Optimization of population frequency cutoffs for filtering common germline polymorphisms from tumor-only next-generation sequencing data. J Mol Diagn 21: 903-912, 2019.
63. Sukhai MA, Misyura M, Thomas M, Garg S, Zhang T, Stickle N, Virtanen C, Bedard PL, Siu LL, Smets T, *et al*: Somatic tumor variant filtration strategies to optimize tumor-only molecular profiling using targeted next-generation sequencing panels. J Mol Diagn 21: 261-273, 2019.
64. Hiltemann S, Jenster G, Trapman J, van der Spek P and Stubbs A: Discriminating somatic and germline mutations in tumor DNA samples without matching normals. Genome Res 25: 1382-1390, 2015.
65. Teer JK, Zhang Y, Chen L, Welsh EA, Cress WD, Eschrich SA and Berglund AE: Evaluating somatic tumor mutation detection without matched normal samples. Hum Genomics 11: 22, 2017.